Magazine of Concrete Research
Volume 64 Issue 11

Prediction of FRP debonding using the global-energy-balance approach
Achintha and Burgoyne

Magazine of Concrete Research, 2012, **64**(11), 1033–1044
http://dx.doi.org/10.1680/macr.11.00182
Paper 1100182
Received 03/10/2011; revised 10/01/2012; accepted 17/02/2012

ice
Institution of Civil Engineers
publishing

Prediction of FRP debonding using the global-energy-balance approach

Mithila Achintha
University Lecturer in Structural Engineering, Infrastructure Group, Engineering and the Environment, University of Southampton, Southampton, UK

Chris J. Burgoyne
Reader of Concrete Structures and Head of the Structures Group, Department of Engineering, University of Cambridge, Cambridge, UK

A major research programme was carried out to analyse the mechanism of fibre-reinforced polymer (FRP) debonding from concrete beams using the global-energy-balance approach (GEBA). The analyses developed in the study provide an essential tool that will enable fracture mechanics to be used to determine the load at which FRP plates will debond from concrete beams. This obviates the need for finite-element analyses in situations where reliable details of the interface properties and crack-tip stress fields are not obtainable for an accurate analysis. This paper presents an overview of the GEBA analyses that is described in detail elsewhere, and explains the slightly unconventional assumptions made in the analyses.

Notation

A	cross-sectional area
a	crack length
B	equivalent elastic stiffness
b_p	width of the FRP
E	Young's modulus
F_p	force in the FRP
G_C	fracture energy
G_R	energy release rate
h	beam depth
I	stiffness
K	interpolation coefficient
L	beam span
l_d	crack length
M	moment
W	work
α	equivalent centroid
α_{eff}	centroidal location of a partially cracked section
ε	strain
κ	curvature
Π	potential energy
σ	stress
Subscripts	
I	mode I
II	mode II
app	applied
cr	critical
eff	effective
ext	external
fc	fully cracked
sys	system
un	uncracked

Introduction

A comprehensive study of the debonding of fibre-reinforced polymer (FRP) plates from concrete beams using the global-energy-balance approach (GEBA) has been undertaken; many of the concepts used have been described elsewhere (Achintha and Burgoyne, 2008, 2009, 2011a, 2011b). This paper summarises the overall logic of the model.

A high stress may cause a crack to form near the interface between the concrete and the FRP, but that crack will only propagate if more energy is thereby released than it takes to form the new fracture surfaces. It is thus a fracture-mechanics problem, not a stress-analysis problem. It should be noted that manufacturers have now developed adhesives that are sufficiently tough that, if they are used correctly, debonding usually takes place in the concrete cover between the FRP and the tension steel reinforcement bars (Figure 1(a)). The application of GEBA analysis to the study of debonding of FRP plates from concrete beams is a very simple concept, but it requires understanding of some complex mechanics. When a crack extends, the beam loses some of its stiffness; so the load does more work, most of which is stored by an increase in strain energy within the beam. To calculate the energy that is released, these two quantities have to be calculated with a reasonable accuracy. The debonding analyses rely on knowing the fracture energy of concrete (G_C), a parameter that is easy to define but less easy to determine, and one that is rarely assessed in experimental studies. This paper addresses a number of issues that are important in the analysis of debonding of FRP plates: they are controversial and go against accepted wisdom (e.g. the revised moment–curvature model; the location of an effective centroid in beam sections; incorporation of the effect of the FRP on the concrete beam as an external prestres-

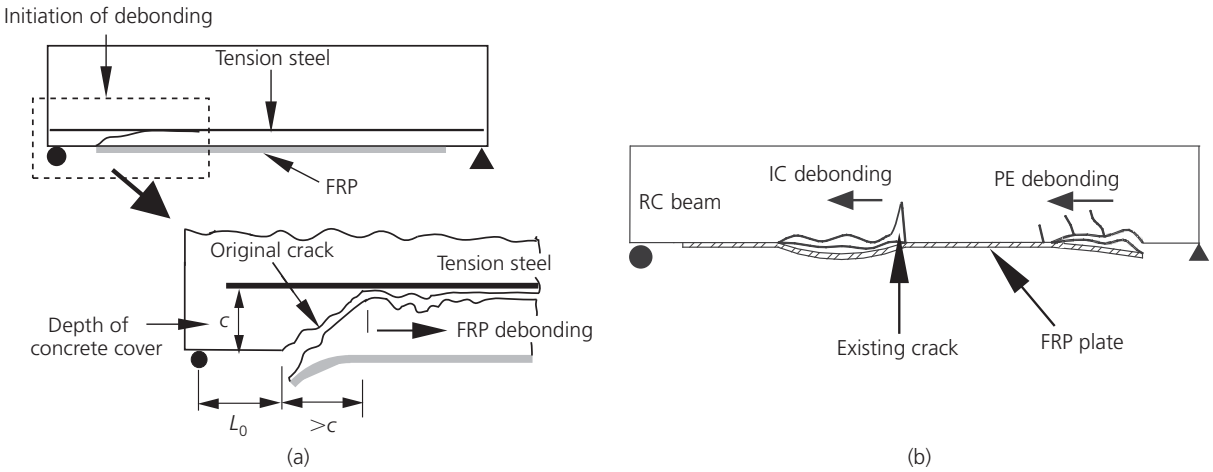

Figure 1. (a) Debonding propagates in the cover zone of the beam. (b) Two modes debonding

sing load; the use of mode I fracture energy; and the absence of an R-curve analysis). The logic of the new model will be explained in more detail below.

Premature FRP debonding hampers efficient use of externally bonded FRP plates in flexural strengthening of concrete beams, and uncertainty about the governing mechanisms means that there is no reliable theory that can be applied by designers. The fracture-mechanics-based finite-element (FE) methods often used in the literature to determine failure load were mostly based on the pioneering theory of Hutchinson and Suo (1992), which was intended for the analysis of interface debonding in thin-layered elastic materials. However, because of the large fracture process zone (FPZ) associated with a crack in concrete, the concrete–FRP interface cannot be modelled using the concepts of linear-elastic-fracture mechanics (Karihaloo, 1995). Non-linear FE models with a 'special' element to model the FPZ (e.g. 'spring' type elements to incorporate the effects of the cohesive forces) may be used to analyse FRP debonding. However, the FE simulations require far more detail of the interface properties (such as the distribution of voids in the interface between the adhesive and the concrete) than will ever be available to designers. In a FE model the crack path must be known a priori; a crack follows the path of least resistance around or through the aggregate, but reliable estimates for possible fracture path cannot be made. Alternatively, the use of smeared-crack FE models (Wang and Zhang, 2008) avoids the need to model discrete cracks, but this method fails to model debonding, which is triggered by the growth of a dominant crack. Elements with dimensions significantly smaller than the size of the aggregate are needed in FE models to obtain consistent results. However, at this length scale, concrete does not behave as a homogeneous material.

The present authors have earlier developed a more physically based fracture mechanics model that represents energy balance requirements, rather than an unreliable analysis of the crack-tip stress field. The GEBA model is based on governing parameters that can be reliably determined and the model is able to analyse all modes of FRP debonding. Methods to determine the energy states in beams and fracture energy of concrete to a reliable accuracy were developed, and the use of these results in the debonding model predicted results that match with test data reported in the literature (Achintha and Burgoyne, 2011a).

The evaluation of energy states in cracked concrete beams using the stress–strain (σ–ε) behaviour over the whole beam is very complex, so in the present model a simpler integration of moment–curvature (M–κ) is used, but even determining the curvature κ is complex. Branson's model (Branson, 1968) was conceived only for beams with steel reinforcement, and only up to the point where the steel yields. When external FRP is added there is an additional layer of reinforcement with different bond characteristics, so it is incorrect to incorporate the FRP as a second layer of steel reinforcement in the Branson model. The M–κ model also has to be applicable after the steel has yielded because that is why the beams needed strengthening in the first place. The present paper shows how these issues have been addressed.

In recently developed non-linear fracture mechanics models (e.g. Wang and Zhang, 2008), the results of shear-lap experiments were used to derive the fracture energy of concrete (G_C) in strengthened beams. However, the tests do not provide an accurate estimate of G_C because the interface of a strengthened beam actually fails in tension (mode I cracking), whereas results of shear-lap tests provide an estimate for shear mode (mode II) fracture energy (G_{CII}), which is about 20 times larger than that for mode I (G_{CI}) (Achintha and Burgoyne, 2011b). As a further complication, debonding occurs in the narrow concrete cover,

between the FRP and the steel bars (Figure 1(a)), hence it is unlikely to develop the FPZ fully. Thus, the value of G_{CI} to be used in a debonding analysis should be that obtained from small-scale test specimens.

The plate end, and zones where widening of flexural cracks cause interface flaws, are most susceptible to the initiation of debonding; the two modes are referred to as 'plate-end' (PE) and 'intermediate-crack-induced' (IC) debonding, respectively (Figure 1(b)). PE debonding initiates from the vicinity of the FRP end and propagates towards the mid-span of the beam, whereas IC debonding initiates at a high-moment zone and propagates towards a low-moment zone. Experimental studies reported in the literature suggest that PE debonding is the likely failure mode of most strengthened beams (Teng *et al.*, 2002), and hence a number of studies have investigated the effectiveness of the use of plate-end anchoring systems (e.g. FRP jackets; Quantrill *et al.*, 1996) and the use of long FRP plates right up to the beam end (e.g. Ross *et al.*, 1999) as methods to resist PE debonding. Although the methods improved the strength and the ductility of beams, the fact that PE debonding still takes place may be due to the stress concentrations developed due to the anchoring devices. The use of long FRPs right up to the beam end eliminated PE debonding, but this can lead to premature IC debonding. The present GEBA model can predict failure loads of both modes of debonding.

GEBA model

Using the concept that 'the current state of a system will be at a position of minimum total potential energy', the GEBA model determines that debonding will occur if the energy available for a potential small extension of an existing interface crack exceeds the energy needed to form the required new fracture surfaces – that is, if the energy release rate (G_R) (energy release per unit extension of a crack of unit width) associated with the crack exceeds the fracture energy of concrete then the crack will propagate. How the initial crack developed up to the current state is immaterial in the model and it is sufficient to assume that flaws of the relevant size are likely to exist. The model can be used to determine the shortest crack that triggers failure at a given load or the failure load of a beam with a crack of known length.

The determinations of G_R and G_{CI} precisely, either theoretically or experimentally, are complex; appropriate methods to calculate both parameters will be discussed below. The G_R associated with a given crack can be determined by considering the energy changes that take place in the beam during a small crack extension. However, the use of M–κ relationships determined on the assumptions that the section is uncracked (i.e. concrete is fully effective in tension) underestimates the energy state, while if the beam is assumed to be fully cracked (i.e. no tensile contribution from concrete) the energy state is overestimated. Various tension-stiffening models exist, although these were primarily developed to calculate the deflections of conventional reinforced concrete (RC) beams (i.e. beams with internal steel reinforcement only). Branson's model indirectly incorporates the effects of tension-stiffening in cracked beams by defining an effective stiffness and the model has been widely verified in the literature. In the present work the model has been modified to take account of the effects due to the FRP, and the use of a new model to determine energy states of strengthened beams is discussed below.

A fracture propagates in the concrete substrate, so it is necessary to know the G_C of the concretes from which the beams are made. In different modes of fracture (opening, shear, or mixed-mode), different stress fields will develop in the FPZ, so it is necessary to determine whether G_C corresponds to the correct fracture mode. The study has shown that the FRP force, acting with an eccentricity with respect to the tip of the shear crack that triggers PE debonding, causes a dominant tension in the crack tip, and hence debonding is triggered by crack opening (Figure 2(a)). In IC debonding, the FRP cannot slide parallel to the beam because it is fixed at the rear end of the unbonded zone, but it can move away from the surface (Figure 2(b)). Thus, in both modes, debonding propagates locally as a mode I crack in concrete. The incorporation of G_{CI} in the GEBA model provided results that match with test data reported in the literature. The present paper explains why particular values for G_{CI} have been chosen.

Mechanism of FRP debonding

PE debonding occurs when an interface crack forms due to the widening of a shear crack in the vicinity of the FRP end, whereas IC debonding is triggered by an interface crack formed due to the widening of a critical flexural crack in the high-moment zone (Figure 1(b)). Shear and peeling stress concentrations develop due to geometric restraints and, due to the relative vertical movements of the faces of the critical shear/flexural crack, trigger further propagation of the already-formed interface crack, causing separation of FRP from the beam. The whole concrete cover of the beam usually separates during PE debonding, whereas a concrete layer of only a few millimetres thick separates during IC debonding. This observation has led some researchers to analyse PE debonding as a shear failure of the concrete beam and IC debonding as an interface failure (e.g. Teng *et al.*, 2002). The present authors assert that both modes are essentially fractures in the concrete substrate and the difference in the fracture path is due to the effect of the difference in the magnitude of force in the FRP (F_p) in the corresponding locations. The principal interfacial stress in the vicinity of the interface crack will be at about 45° to the interface, and thus it is expected that the crack will move into the beam. PE-debonding cracks move up to the level of tension steel bars and the final failure occurs at this level. However, during IC debonding, the large force F_p that acts eccentrically to the crack tip takes the crack back down towards the interface, and debonding propagates in the concrete beam just a few millimetres above the interface.

The present GEBA model predicts FRP debonding by comparing two governing parameters, the G_R and the G_{CI} values of the concrete of which the beam is made. An essential first stage of

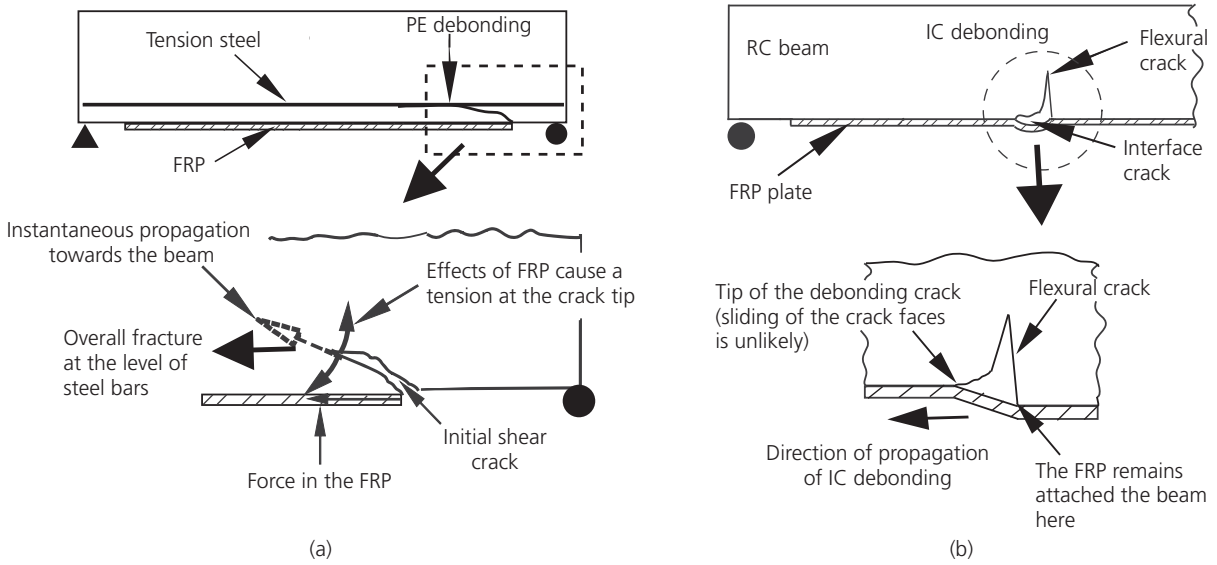

Figure 2. (a) The eccentricity in the FRP force with respect to the tip of the shear crack causes a dominant tension in the crack tip. (b) In IC debonding, the FRP cannot slide parallel to the beam because it is fixed at the rear end of the unbonded zone

the calculation of G_R associated with a crack is the determination of the energy state of the beam at a given applied load, derived using the M–κ model that is discussed below.

Moment-curvature analysis using Branson's model

Although the analysis of a RC beam section with the assumptions that the section was uncracked or fully cracked is straightforward, an accurate M–κ analysis of a partially cracked section while including tension-stiffening effects of cracked concrete is not trivial. Branson's model (Equation 1) defines an effective stiffness (I_{eff}) of a cracked beam section as an interpolation between the values of the uncracked (I_{un}) and fully cracked (I_{fc}) sections. (I_{un} and I_{fc} can be determined to an acceptable accuracy from an elastic and a cracked-elastic analysis, respectively.) The interpolation coefficient (K in Equation 1) takes account of the current cracking level of the section and is defined as the ratio between the moment that causes the first flexural crack in the section (M_{cr}) and the current applied moment (M_{app}). The model has been validated against test results of deflections of RC beams and, with appropriate modifications, against test results of prestressed concrete beams (Branson and Trost, 1982).

$$1. \quad I_{eff} = KI_{un} + (1 - K)I_{fc}$$

where $K = (M_{cr}/M_{app})^4$. I_{eff} in Equation 1 is the effective second moment of area of the equivalent transformed concrete section of modulus E_c, so curvature of the section (κ) can be determined as in Equation 2.

$$2. \quad \kappa = \frac{M_{app}}{E_c I_{eff}}$$

A modified Branson's model for strengthened beams

In a strengthened beam, the M–κ relationships of uncracked/fully cracked sections can be determined as those of a conventional beam while taking account of the force in the FRP (F_p). The objective is to use Branson's concept to determine stiffness and hence κ in a partially cracked beam section. However, the original model will need modifying here because it is not correct to consider FRP as a second layer of internal steel reinforcement. The earlier work by the present authors (Achintha and Burgoyne, 2009) has shown that, if the effect of F_P is incorporated as an external force on the RC beam alone, the analyses can be simplified conceptually since it allows the use of Branson's model to analyse the RC beam portion as a conventional beam (Figure 3(a)). However, this requires analysing the RC section for a combined action of an axial force and moment. At any given location along the beam, the moment due to the applied load is generally known (M_{app}). This acts on the combined beam section (i.e. RC beam section + FRP plate). The portion of the applied moment that is resisted by the RC section alone (M_{eff}) can be determined if the location of the centroid is known. The energy in the RC beam can then be determined as $\int_L M_{eff}\kappa\,dx + \int_L F_p\varepsilon_0\,dx$ (where κ is curvature, ε_0 is strain in the beam section at the centroidal location, and L is beam span). The FRP also stores some energy and the calculation of it is trivial since it is assumed to be linear elastic. Calculation of the beam's

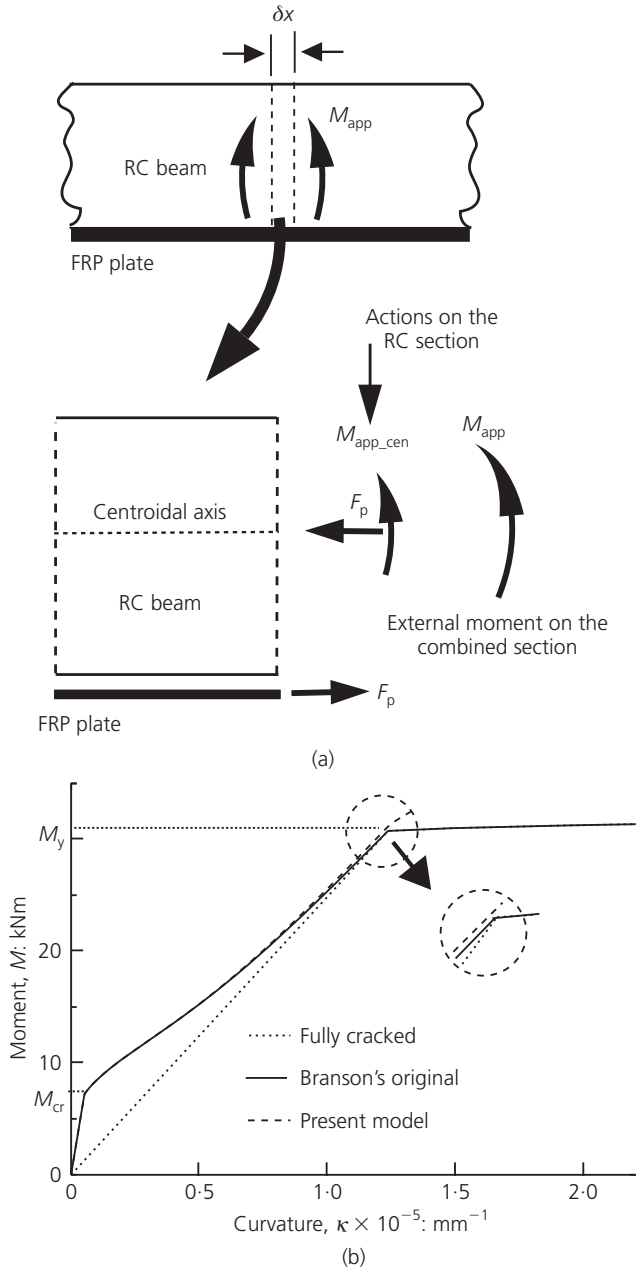

Figure 3. (a) Taking the effect of FRP as an external prestressing force allows the use of Branson's model. (b) In a conventional beam, the assumption of the fully cracked state at M_y does not cause significant changes to the results but avoids a discontinuity at M_y

energy state in this way requires knowledge of the section's centroid and the determination of it will be discussed below.

Complexities over conventional Branson analysis

Branson's model applies to RC beams subjected to pure bending and the modifications required to analyse a section subjected to an axial force and moment are discussed below.

Force in the FRP

Branson's model is concerned only with stiffness and is not used to determine the strains in the beam, which are assumed to be adequate because separate checks (permissible stress/section strength) would be performed. However, in a strengthened beam, if the FRP is bonded to the beam section, then the strain in the FRP is locally compatible with that in the RC section, and if the FRP is partly unbonded over a zone, then over the unbonded zone the extension of the FRP is compatible with that of the RC beam (Achintha and Burgoyne, 2009). Thus, the model requires the satisfaction of a compatibility condition between the FRP and the concrete, which means that strong assumptions need to be made about the strains, and hence stresses, in the beam section; these have to be determined from the effective stiffness. As a result, F_p at a given location in the beam span cannot be known a priori, so it is treated as a variable and determined numerically using a least-squares method. Once an accurate value for F_p is known, all other parameters may be evaluated (Achintha and Burgoyne, 2009).

Location of equivalent centroid

It is impossible to find an exact axis in a cracked RC beam section that satisfies the requirements of the centroid in a linear elastic analysis (i.e. $F_p = \int_A \sigma \, dA$ and $M_{eff} = \int_A \sigma y \, dA$, where A is the cross-sectional area and y is the distance from the centroid; strain energy is given by $\int_L M_{eff} \kappa \, dx + \int_L F_p \varepsilon_0 \, dx$). The concept of 'equivalent centroid' (α) was thus developed for strengthened beam sections such that it would allow the separation of M_{eff} and F_p approximately, and hence the determination of the energy state in the usual way to an accuracy good enough to be used in the debonding analyses. For uncracked and fully cracked sections the σ–ε distributions are reliably known from respective section analyses, and hence the relevant α (α_{un} and α_{fc}, respectively) can be determined by considering the equivalent transformed sections, while taking account of the secant modules of non-linear materials. The centroidal location of a partially cracked section (α_{eff}) will then be interpolated between the respective α_{un} and α_{fc} using Branson's concept; this analysis is presented elsewhere (Achintha and Burgoyne, 2009). It should be noted that the materials are non-linear, and hence the location of α changes with the applied load. Thus, there is no fixed centroid that is a section property.

Modified interpolation coefficient

When the amount of cracking increases, the tension-stiffening effects eventually become ineffective. In Branson's model, however, the stiffness in the section becomes asymptotic to the fully cracked state but never reaches it. That model was intended to represent sections at working loads and well below yield of the steel bars. However, the fully cracked state will be reached in strengthened beams. In the present model, it was assumed that a beam section will be fully cracked at the moment that causes first yielding of tension steel (M_y); and the interpolation coefficient (K_p) is determined by considering the magnitudes of M_{cr}, M_y and M_{app} (Achintha and Burgoyne, 2009). This modification does not

cause significant changes to the predictions from the original model for conventional beams but avoids a discontinuity in stiffness when the steel yields (an example is shown in Figure 3(b)). As a further complication, because of the presence of the axial load, the moment acting on the RC section alone depends on the choice of the axis about which it acts. The obvious choice would be the centroid, but this is not at a fixed location, either along the beam or as the loading increases. To avoid complications, it was decided to use a fixed axis about which to calculate the effective moment used to determine the interpolation factor K_p; the mid-depth axis of the beam was chosen, the corresponding moments are $M_{cr\text{-}m}$, $M_{y\text{-}m}$, and $M_{eff\text{-}m}$, respectively (Equation 3).

$$3. \quad K_p = \left(\frac{M_{cr\text{-}m}}{M_{eff\text{-}m}}\right)^4 \left[1 - \left(\frac{M_{eff\text{-}m} - M_{cr\text{-}m}}{M_{y\text{-}m} - M_{eff\text{-}m}}\right)^4\right]$$

Equivalent elastic stiffness

As discussed previously, M_{eff} and κ of uncracked and fully cracked sections can be directly determined from respective section analyses. The new model is used to determine effective stiffness and hence κ of partially cracked sections. Since the model is to be applied to sections where the material nonlinearity needs to be taken into account, the cracked-elastic analysis used in the Branson model is not applicable. Since the Young's modulus of concrete is no longer fixed, there is no value in defining an equivalent second moment of area. Instead, an equivalent elastic stiffness (B) is defined in place of the product of E_c and I_{eff} used in Branson's model. The values of B for uncracked and fully cracked sections (B_{un} and B_{fc}, respectively) can be determined from the direct section analyses. For a partially cracked section, the relevant B_{un} and B_{fc} are first calculated, and that of the actual section (B_{eff}) is then interpolated (Equation 4). The location of α_{eff} and hence M_{eff} of the section is known, so combining M_{eff} with B_{eff} the κ of the section can be determined (Equation 5).

$$4. \quad B_{eff} = K_p B_{uc} + (1 - K_p) B_{fc}$$

where K_p is from Equation 3.

$$5. \quad \kappa = \frac{M_{eff}}{B_{eff}}$$

Validation of the present M–κ model

The new M–κ model was applied to several sets of beam tests reported in the literature and it was found to be accurate enough for a model of RC beams (Achintha and Burgoyne, 2009). All the beams analysed in the study were tested as simply supported beams and a large database of specimens, including a variety of material/geometric properties, was investigated. The model was also used to determine strain and deflection profiles of strengthened beams. Single examples of M–κ and strain profile comparisons are shown in Figure 4.

Figure 4(a) shows an M–κ comparison for beam A3.1 tested by Spadea *et al.* (1998). It shows that the model can accurately predict behaviour for all uncracked, partially cracked, and fully cracked regimes. The predicted M_{cr} and M_y are marginally higher than those actually noted, which may be due to the overestimation of the concrete tensile strength or the yield strength of steel. The small variations in the predicted stiffness may be due to a slight overestimate of the stiffness of concrete. Comparisons with the measured strains in the FRP at three different locations in beam CB4-2S tested in four-point bending by Alagusundaramoorthy *et al.* (2003) are shown in Figure 4(b). Locations SG6, SG4 and SG3 indicated in Figure 4(b) correspond to positions in the constant-moment zone, at the centre of one of the shear spans, and at a distance of one quarter of the shear span from the beam end, respectively. Good correlations can be noted in all cases.

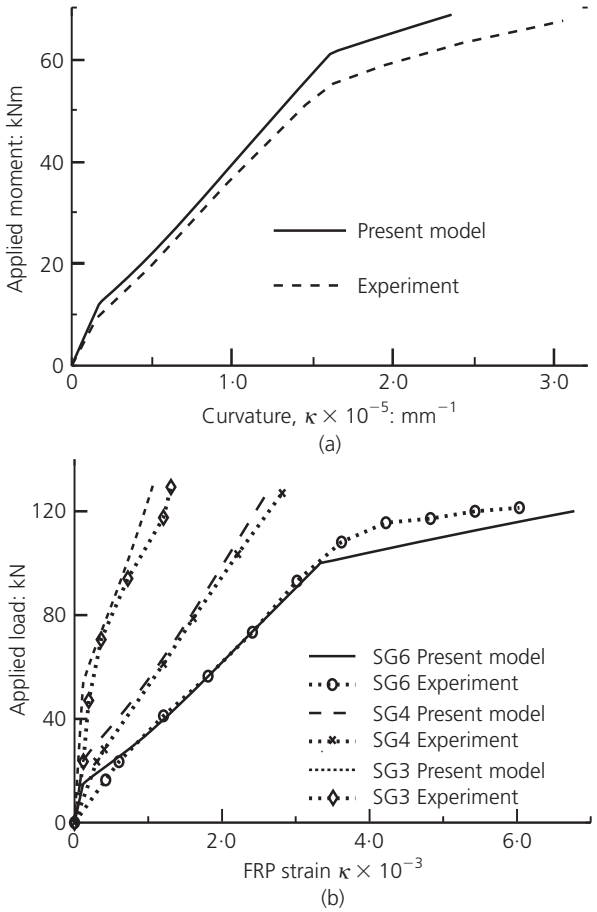

Figure 4. (a) M–κ comparison for beam A3·1 (Spadea *et al.*, 1998). (b) FRP strain comparisons along the span of beam CB4-2S (Alagusundaramoorthy *et al.*, 2003)

Thus, not only does the model correctly predict the curvatures, but it also correctly predicts the neutral axes, from which it can be assumed that the strain profile will be correct.

Determination of energy release rate

In the GEBA model the G_R associated with a small extension of a given interface crack is to be compared with G_{CI} to decide whether the crack will propagate. The present $M-\kappa$ model is used to determine G_R at a given applied load. When the crack extends, the beam loses some of its stiffness, so work is done by the external loads. The curvature increases in the beam, storing some of this extra work as strain energy, but some is left over to cause the crack to propagate. Thus, according to the global energy balance of the system, the G_R is the rate of change of the system's total potential energy (Π_{sys}) with respect to the crack length (a) (Equation 6) (Π_{sys} = potential energy in the applied loads (W_{ext}) + work done on the beam (W_{beam})).

$$G_R = -\frac{1}{b_p}\left(\frac{\partial \Pi}{\partial a}\right) = -\frac{1}{b_p}\left(\frac{\partial W_{beam}}{\partial a} + \frac{\partial W_{ext}}{\partial a}\right) \quad (6)$$

where b_p is the width of the FRP.

It should be noted that when a RC beam bends, a part of the energy put into the beam by the loads is dissipated in cracking and steel yielding, and the rest is stored as the beam's strain energy. Therefore, in the analysis of FRP debonding, it is not correct to determine G_R as the rate of change in the beam's strain energy, as is usually done in a conventional linear-elastic-fracture mechanics analysis, where the change in the total potential energy in the system is solely used to create the new fracture surfaces and to increase strain energy in the beam.

The method used to calculate G_R

In order to focus on the basic mechanics, the calculation of G_R in a simply supported beam is discussed below. (The procedure would need modifying if a statically indeterminate beam were to be analysed, when the distribution of moments caused by applied loads would change as the beam's stiffness changed during crack extension.) G_R is determined as the change in the system's total potential energy ($\Delta\Pi$) per unit area of new interface crack (G_R has the units N/mm). Due to the crack extension, the beam softens, but not uniformly. Over most of the length of the beam the curvature (κ) and hence the strain energy remain unchanged; it is only the region of the beam near the crack tip where significant changes in curvature occur. G_R associated with PE debonding is determined by considering the energy and κ changes take place in beam segments within the plate-end transfer zone (BE in Figure 5(a)); for IC debonding κ changes take place in the unbonded zone and the two transition zones (CF in Figure 5(b)). Outside these zones, the FRP is fully bonded to the concrete, so if the load does not change during the crack extension, the moment and hence the curvature remains constant.

It is important to know the length of the transition zone. A simplified model, based on the more rigorous interfacial stress analysis of Täljsten (1997), was used to determine the distribution of F_p in the plate-end stress transfer zone and also that in the transition zones associated with an IC debonding crack (Achintha and Burgoyne, 2008). The results show that the length of each of

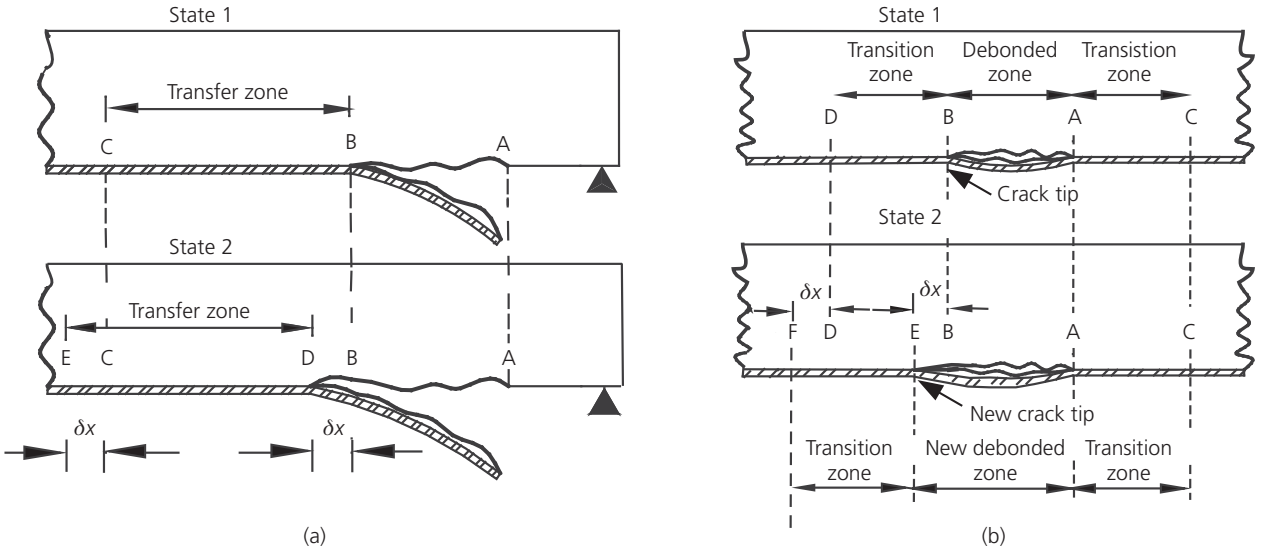

Figure 5. Energy release zones: before (state 1) and after (state 2) small (δx) crack extension: (a) PE debonding and (b) IC debonding extension

these stress-transfer zones is about 30 times the thickness of the FRP for most FRP/adhesive/concrete combinations; this value is used in all subsequent analyses.

Calculation of G_R

The objective is to determine the $\Delta\Pi$ (i.e. the sum of the additional work done on the beam (ΔW_{beam}) and the change in the potential energy of externally applied loads (ΔW_{ext}) due to the small crack extension) by using the present M–κ model. Only the changes in the energy state and κ in the critical zone (Figure 5) are considered. The critical zone is first divided into segments 1 mm long and the additional work done (δW_{beam}) and the change in curvature ($\delta\kappa$) in each segment after the assumed crack extension are calculated as shown below. The δW_{beam} in each segment is then summed to obtain ΔW_{beam}. By numerically integrating $\delta\kappa$ of individual beam segments, the change in deflection profile and hence ΔW_{ext} can be calculated.

Calculation of ΔW_{beam}

Due to the crack extension, both the effective moment (M_{eff}) and the axial force (F_p) in RC segments alter and there will also be a change in the strain energy in the FRP. According to the present M–κ model, the δW_{beam} in a beam segment consists of three components: additional work done in the RC section due to the change in M_{eff} (δW_M); additional work done in the RC section due to change in F_p (δW_F); and change in strain energy in the FRP (δW_{FRP}). Figure 6(a) shows the changes in all three action–deformation relationships in a beam segment, with the assumption that all have increased during the transformation. All M, κ, F_p and ε_0 values of the segment before and after the crack extension (i.e. states 1 and 2, respectively) can be calculated from the M–κ model, and hence δW_{beam} and ΔW_{beam} can be determined (Equation 7).

$$\delta W_{beam} = \delta W_M + \delta W_F + \delta W_{FRP}$$

$$\text{and } \Delta W_{beam} = \sum_{\text{critical zone}} \delta W_{beam} \quad (7)$$

Calculation of ΔW_{ext}

By numerically integrating $\delta\kappa$ in the beam sections within the critical zone, the change in beam's deflection profile (Δ_{dis}) and hence δW_{ext} can be determined as in Equation 8 (Figure 6(b)).

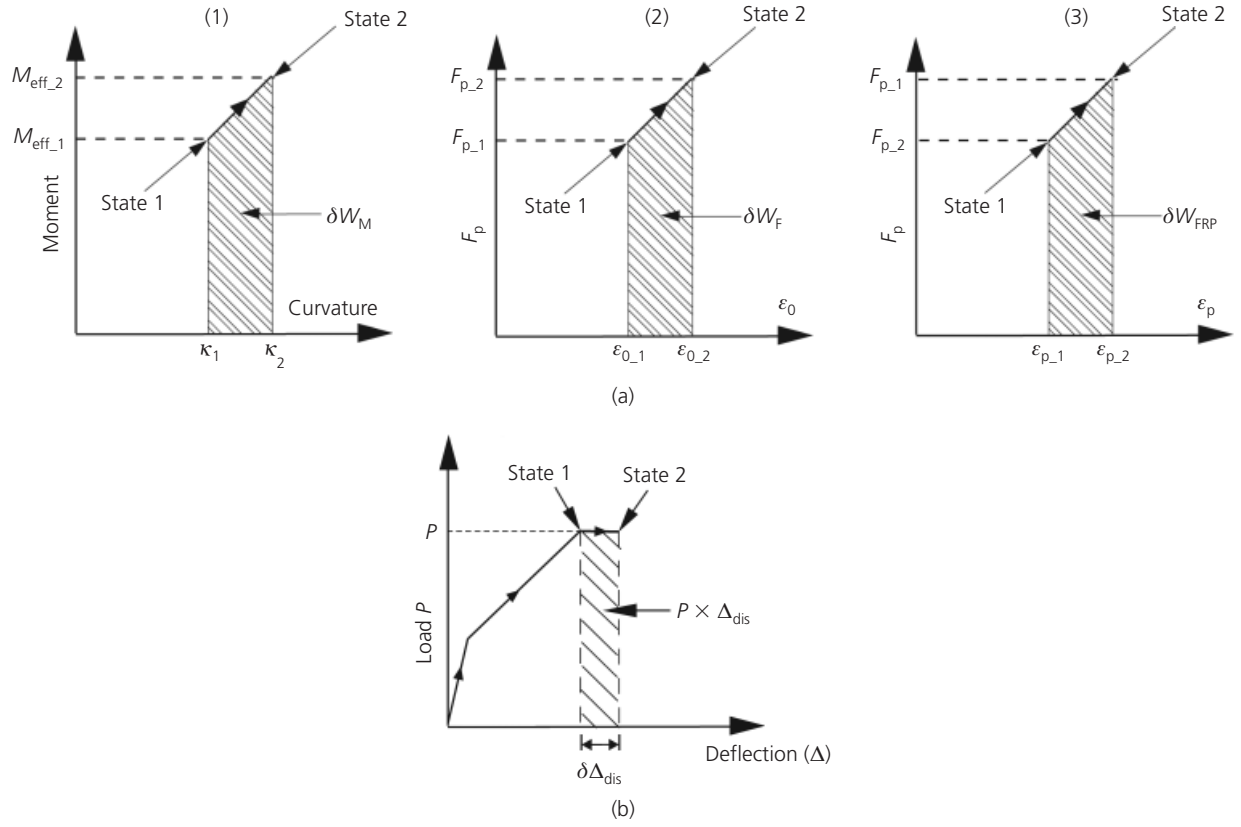

Figure 6. (a) Changes in the actions effective on a beam segment due to the crack extension: (1) moment, (2) axial force in the concrete beam section, (3) FRP plate. (b) Change in potential energy of the applied loads

$$\Delta W_{\text{ext}} = \sum_{\text{for all loads}} P\Delta_{\text{dis}} \quad (8)$$

where P is the applied load. Finally G_R can be calculated (Equation 9):

$$G_R = -\frac{1}{b_p}(\Delta W_{\text{beam}} + \Delta W_{\text{ext}}) \quad (9)$$

(typically, $\Delta W_{\text{ext}} < 0$).

Accuracy of G_R calculated from the M–κ model

Lack of a reliable σ–ε model to incorporate tension-stiffening means that it is impossible to verify the results of the M–κ model generally. However, if a case is considered in which the debonding takes place either in a region that is completely uncracked or one that is fully cracked, the G_R value can be determined from σ–ε integration, so the error in the results calculated from M–κ integration can be investigated. Figure 7(a) shows the G_R calculated from M–κ and σ–ε analyses for an interface crack that initiated IC debonding in a typical beam, with all the sections in the critical zone in the fully cracked state. Figure 7(b) shows that G_R calculated from the M–κ model agrees well with that from σ–ε analysis with about 5% error, which is well below the variance of about ±10% usually associated with experimentally determined G_{CI} (Karihaloo *et al.*, 2003). Analysis of other beams shows similar results.

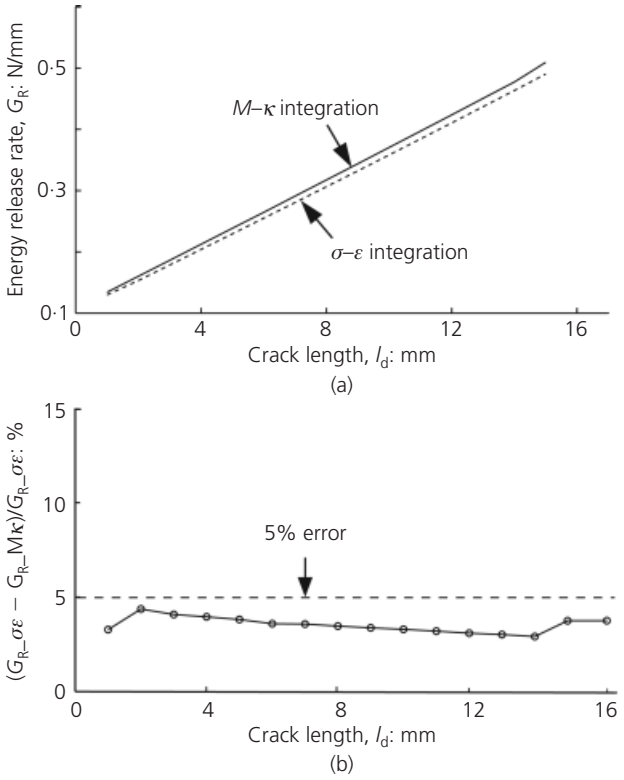

Figure 7. (a) G_R estimates from σ–ε and M–κ analyses. (b) Percentage error in G_R calculated from M–κ integration

Effect of tortuous crack paths

Due to the material heterogeneity and the complex crack-tip stress field, debonding does not propagate on a unique plane, so the G_R calculated as above represents the G_R per unit area of crack projected onto the horizontal plane. Nevertheless, G_R calculated this way can still be compared with G_{CI}, which is either experimentally determined or based on approximate simplified models, both of which inevitably include accounts for tortuous crack paths and also for the development of microcracks. The GEBA model only requires a reliable estimate of G_{CI}, which is usually available, whereas a FE-based analysis would require accurate details of crack path and the microcracks, all of which are difficult to know with any certainty.

Interface fracture energy

The GEBA model relies on knowing the fracture energy of the concrete of which the beam is made. A combination of normal and shear stresses will be present in the vicinity of an existing interface crack. It might be supposed therefore that a mixed-mode fracture energy would be relevant. However, the present study has shown that in PE debonding the FRP force, acting with an eccentricity with respect to the tip of the original shear crack, causes the crack to propagate by opening (Figure 2(a)). In IC debonding, the FRP cannot slide parallel to the concrete because it is fixed at the rear end of the unbonded zone (Figure 2(b)). Thus, despite mixed-mode loading present in the crack tip, because of the relatively high shear fracture resistance of concrete, and also since large crack plane separations are required to activate shear fracture mechanisms, it is appropriate to assume that fractures that trigger either mode of FRP debonding are dominated by G_{CI}, which is much less than G_{CII}.

Invariance of the fracture energy in FRP debonding

When a fracture develops in a large block of concrete, it is possible for the FPZ to develop fully. However, FRP debonding propagates in the narrow zone of concrete, between the FRP and the steel bars in the beam; both the steel and the FRP are bonded to the concrete ahead of the crack, so the strain in the concrete is limited. The effect is that the FPZ is of limited extent. Furthermore, the FPZ cannot be influenced by the length of the crack, because it is not possible for any deformation of the FRP (the concrete being sensibly rigid) to change the state ahead of the crack tip. Thus, the size of the FPZ ahead of the crack tip remains unchanged (Figure 8), and hence the fracture energy must be independent of the crack length.

The corollary of this argument is that the fracture energy to be used in a debonding analysis should be the value obtained from small-scale test specimens, or from the initial stages of tests on larger specimens when the FPZ has not fully developed. This is consistent with earlier analyses of FRP debonding that have

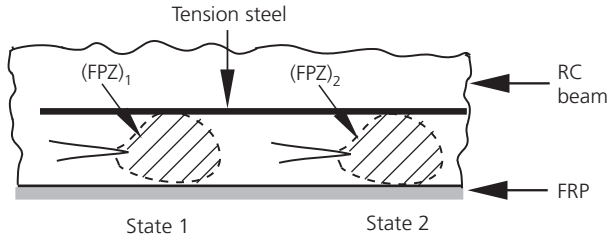

Figure 8. The size of the FPZ remains constant as debonding propagates

shown that interface cracks 20–30 mm and 2–5 mm long cause PE and IC debonding, respectively (Achintha and Burgoyne, 2011a). Details of experimental and theoretical investigations of G_{CI} of concretes are presented in Achintha and Burgoyne (2011b); the methods by which the G_{CI} values of the beams quoted in that study were determined and the values that result are briefly discussed below.

Determination of G_{CI}

No accepted direct method exists for the analysis of stress against crack-opening relations in the FPZ, which is required to determine G_{CI}. Although a reliable estimate for G_{CI} of a given concrete can be determined from tests, in the reported studies of FRP debonding the relevant G_{CI} values were not measured, so it is necessary to decide on values that can be used in the GEBA analysis. Simplified models reported in the literature, which can be used to estimate G_{CI} of a given concrete based on more readily known properties of the concrete (compressive strength, size and type of the aggregate) were used in the present work to estimate G_{CI} of the concretes used in the beams being analysed (Achintha and Burgoyne, 2011b).

Estimation of G_{CI} using simplified models

Simplified models determine G_{CI} as energy required to open the tip of a traction-free crack to a critical value where there are no stress transfers across the crack. The stress against tip-opening (σ_I–w_I) relationship is referred to as the tension softening response and is usually represented by a bi-linear or a polynomial form. In the models quoted in the literature, the governing parameters of the σ_I–w_I curve are represented in terms of tensile strength of concrete (f_t), and the type and size of the largest aggregate in such a way that the area under the softening curve agrees with an estimate of G_{CI} obtained from experiments. These models were used to estimate G_{CI} of the concretes used in the beams being considered in the study.

G_{CI} values used in the debonding analyses

The GEBA-based FRP debonding analysis was applied to several sets of beam tests reported in the literature (Achintha and Burgoyne, 2011a). The compressive strength of the concretes (f'_c) used in the beams being tested were in the range 30–55 N/mm^2; crushed aggregates of 20 and 10 mm and 10 mm rounded aggregates were used in the mixes (the complete database can be found in Achintha and Burgoyne, 2011b). The G_{CI} values of the beams under consideration were calculated from concrete data quoted by the experimenters, according to the bi-linear tension-softening models of Guinea *et al.* (1994) and Gustafsson and Hillerborg (1985); and by the polynomial model of Reinhardt (1985); and also using the empirical model of Bažant and Becq-Giraudon (2001). The results show that for a given concrete, the predictions from the models are very similar. The f'_c of the concretes did not vary significantly, so the variations in G_{CI} of the beams depend mainly on aggregate properties (Achintha and Burgoyne, 2011b). Based on the model predictions, G_{CI} values of mixes with crushed aggregates of 20 and 10 mm and 10 mm rounded aggregates were assumed to be 0·15, 0·10 and 0·07 N/mm, respectively. These values agree with experimentally noted G_{CI} values quoted in the literature for concretes with similar properties (e.g. Karihaloo *et al.*, 2003). It should also be noted that the experimentally determined G_{CI} values were often associated with a scatter of about 10%.

Results of FRP debonding analyses

A large database of beam specimens was investigated, including a variety of material and geometric properties, and also covering beams that failed in all possible modes of FRP debonding. Comparisons made in this study (Achintha and Burgoyne, 2011a) have shown that the incorporation of G_{CI} determined as above provides predictions that match the experimental results. An example for PE debonding and one for IC debonding are shown below.

Example: PE debonding

PE debonding initiates due to the formation of a dominant shear crack near to the FRP end. It was assumed that the crack propagates along a direction at 45° to the interface up to the level of the steel bars (the real direction of propagation varies slightly from this but it should not have a significant effect on the results), and therefore it was contended that the 'effective' plate end location (L_{0_e}), just prior to the initiation of debonding, should be located between L_0 and a further cover distance (c) into the beam (Figure 9(a)). The G_R values associated with L_{0_e} values in the range $L_0 - 2c$ and $L_0 + 2c$ were determined and compared with G_{CI} (including a ±10% variation in G_{CI}) to decide whether debonding is possible at the observed failure load (P_f).

Figure 9(b) shows the variation in G_R against L_{0_e} for beam pair F9 and F10 selected from the study of Fanning and Kelly (2001) ($L_0 = 500$ mm and $c = 30$ mm). The G_{CI} of the concrete with 20 mm crushed aggregate was assumed to be 0·15 N/mm. The figure shows that taking L_{0_e} to be 10 mm higher than the actual L_0 (i.e. $L_0 < L_{0_e} < L_0 + c$), the P_f predicted from the model compares well with the P_f observed in the experiment. The figure also shows that, at the observed P_f, any L_{0_e} shorter than the L_0 could not cause PE debonding. The results further show that loads 10% higher or lower than P_f are, respectively, too strong or too weak to cause failure (Figure 9(b)). Thus, the results of the present analyses match with the observed P_f and failure mode.

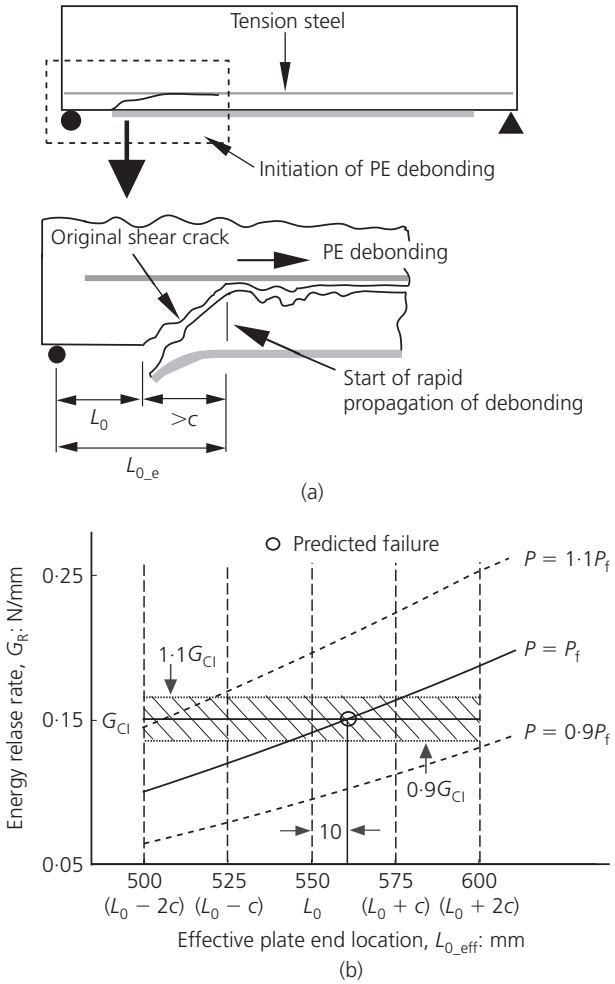

Figure 9. (a) Location of the effective plate end (L_{0_e}). (b) G_R against L_{0_e} plots for beam set F9 and F10 (Fanning and Kelly, 2001)

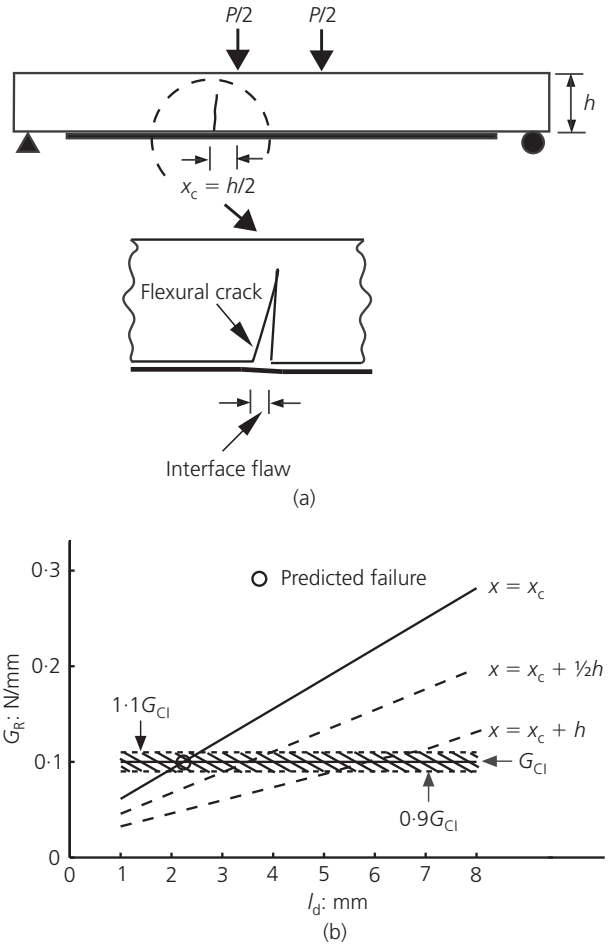

Figure 10. (a) Widening of a critical flexural crack initiates IC debonding. (b) G_R against l_d for different debonding locations (group 1 beam of Ross *et al.*, 1999)

Example: IC debonding

Earlier analyses by the authors have shown that, in four-point bending of beams, interface cracks formed due to widening of flexural cracks located at about a half beam depth (h) away from the loading point (location x_c in Figure 10(a)) cause IC debonding. Analyses of IC debonding noted in a beam set (group 1) reported in Ross *et al.* (1999) are discussed below.

Possible propagation of debonding that is assumed to initiate at the critical location (x_c) and, a further $\frac{1}{2}h$ and h towards the nearest beam end were investigated. Crushed aggregate of 10 mm size was used in the beams, so G_{CI} was assumed to be 0·10 N/mm. The solid line in Figure 10(b) shows the variation in G_R against l_d (crack length) for an interface crack that initiates at x_c, at the observed P_f. Figure 10(b) shows that an l_d of 2 mm would cause failure here; it has been observed that widening of a critical flexural crack forms interface cracks of this magnitude (e.g. Garden *et al.*, 1998). The dashed lines in Figure 10(b) show that, if the debonding initiated at $\frac{1}{2}h$ or h away from the nearest beam end, much longer cracks, of lengths 3·5 mm and 6 mm, respectively, would be required to cause debonding at P_f; these are less likely to occur.

Conclusions

- This study has shown that FRP debonding can be studied by means of a global-energy-balance-based fracture mechanics, which obviates the need for a dubious FE analysis.
- It was necessary to produce a modified form of Branson's model to calculate the energy release during a potential small extension of an existing interface crack.
- It has been shown that FRP debonding can be regarded as a mode I fracture in concrete. The incorporation of this fracture energy in the debonding analyses gives predictions that match the test results reported in the literature.
- The model might form the basis of a parametric study that could identify the parameters that are most important in controlling debonding, and provide guidance about

approximate values of the parameters that should be used when designing beams.

REFERENCES

Achintha M and Burgoyne CJ (2008) Fracture mechanics of plate debonding. *Journal of Composites for Construction ASCE* **12(4)**: 396–404.

Achintha M and Burgoyne CJ (2009) Moment–curvature and strain energy of beams with external FRP reinforcement. *ACI Structural Journal* **106(1)**: 20–29.

Achintha M and Burgoyne CJ (2011a) Fracture mechanics of plate debonding: validation against experiments. *Construction and Building Materials* **25(6)**: 2961–2971.

Achintha M and Burgoyne CJ (2011b) Fracture energy of the concrete–FRP interface in strengthened beams. *ACI Structural Journal* (Preprint available at http:// http://www-civ.eng.cam.ac.uk/cjb/frpdebond/index.html).

Alagusundaramoorthy P, Harik E and Choo CC (2003) Flexural behaviour of RC beams with carbon fibre reinforced polymer sheets or fabric. *Journal of Composites for Construction* **7(4)**: 292–301.

Bažant ZP and Becq-Giraudon E (2001) Statistical prediction of fracture parameters of concrete and implications for choice of testing standard. *Cement and Concrete Research* **32(4)**: 529–556.

Branson DE (1968) Design procedures for computing deflections. *ACI Journal Proceedings* **65(9)**: 730–742.

Branson DE and Trost H (1982) Unified procedures for predicting the deflection and centroidal axis location of partially cracked nonprestressed and prestressed concrete members. *ACI Journal Proceedings* **79(2)**: 119–130.

Fanning PJ and Kelly O (2001) Ultimate response of RC beams strengthened with CFRP plates. *Journal of Composites for Construction* **5(2)**: 122–127.

Garden HN, Quantrill RJ, Hollaway LC, Thorne AM and Parke GAR (1998) An experimental study of the anchorage length of carbon fibre composite plates used strengthened reinforced concrete beams. *Construction and Building Materials* **12(4)**: 203–219.

Guinea GV, Planas J and Elices M (1994) A general bilinear fit for the softening curve of concrete. *Materials and Structures* **27(2)**: 99–105.

Gustafsson PJ and Hillerborg A (1985) Improvements in concrete design achieved through the application of fracture mechanics. In *Application of Fracture Mechanics to Cementitious Composites* (Shah SP (ed.)). Kluwer, Dordrecht, The Netherlands, pp. 639–680.

Hutchinson JW and Suo Z (1992) Mixed mode cracking in layered materials. *Advances in Applied Mechanics* **29**: 63–191.

Karihaloo BL (1995) *Fracture Mechanics and Structural Concrete*. Addison Wesley Longman, Harlow, UK.

Karihaloo BL, Abdalla HM and Imjai T (2003) A simple method for determining the true fracture energies of concrete. *Magazine of Concrete Research* **55(5)**: 471–481.

Quantrill RJ, Hollaway LC and Thorne AM (1996) Experimental and analytical investigation of FRP strengthened beam response: Part I. *Magazine of Concrete Research* **48(4)**: 331–342.

Reinhardt HW (1985) Crack softening zone in plain concrete under static loading. *Cement and Concrete. Research* **15(1)**: 42–52.

Ross CA, Jerome DM, Tedesco JW and Hughes ML (1999) Strengthening of reinforced concrete beams with externally bonded composite laminates. *ACI Structural Journal* **96(2)**: 212–220.

Spadea G, Bencardino F and Swamy RN (1998) Structural behaviour of composite RC beams with externally bonded CFRP. *Journal of Composites for Construction* **2(3)**: 132–137.

Täljsten B (1997) Strengthening of beams by plate bonding. *Journal of Materials in Civil Engineering* **9(4)**: 206–212.

Teng JG, Chen JF, Smith ST and Lam L (2002) *FRP Strengthened RC Structures*. Wiley, Chichester, UK.

Wang J and Zhang C (2008) Nonlinear fracture mechanics of flexural-shear crack induced debonding of FRP strengthened concrete beams. *International Journal of Solids and Structures* **45(2)**: 2916–2936.

WHAT DO YOU THINK?

To discuss this paper, please submit up to 500 words to the editor at www.editorialmanager.com/macr by 1 May 2013. Your contribution will be forwarded to the author(s) for a reply and, if considered appropriate by the editorial panel, will be published as a discussion in a future issue of the journal.